

Carbon nanotubes under electron irradiation: Stability of the tubes and their action as pipes for atom transport

F. Banhart,¹ J. X. Li,¹ and A. V. Krasheninnikov^{2,3}

¹Institut für Physikalische Chemie, Universität Mainz, D-55099 Mainz, Germany

²Accelerator Laboratory, P.O. Box 43, FIN-00014 University of Helsinki, Finland

³Laboratory of Physics, Helsinki University of Technology, P.O. Box 1100, 02015, Finland

(Received 23 September 2004; revised manuscript received 4 May 2005; published 22 June 2005)

The production and migration of carbon interstitials in carbon nanotubes under electron irradiation is studied experimentally and theoretically. It is shown that the threshold for displacing carbon atoms and the defect production rate strongly depend on the diameter of the nanotubes. Multiwalled nanotubes shrink by a loss of atoms and by diffusion of interstitials through the inner hollow in the axial direction. Thus, experimental evidence is given that nanotubes can act as nanoscale pipes for the transport of atoms.

DOI: 10.1103/PhysRevB.71.241408

PACS number(s): 81.07.De, 61.72.Ji, 61.80.Jh

Carbon nanotubes are different from crystalline bulk materials in many respects and have a variety of unusual characteristics that are promising for many applications.¹ It is not only the cylindrically curved graphite lattice of high perfection but also the inner hollow space in single-walled (SWNT) and multiwalled (MWNT) nanotubes that are responsible for their extreme properties, e.g., the ability to uptake a considerable amount of foreign atoms such as hydrogen^{2,3} and lithium.⁴ The efficiency of nanotubes as containers can only be estimated if the diffusivity of atoms in nanotubes is known. Theoretical studies^{4–8} indicate that the atoms inside the hollow cylindrical cores are highly mobile with a diffusivity being much higher than in compact crystalline or amorphous bulk solids. However, the transport of atoms inside nanotubes, a vision that comes involuntarily into mind in view of the striking morphological analogy with macroscopic tubes, is still open to experimental study.

A simple experimental way to investigate the diffusion of atoms inside carbon nanotubes is to inject free carbon atoms into the tubes by irradiating the samples with high-energy particles, e.g., electrons in a transmission electron microscope (TEM). Carbon interstitials are created due to knock-on collisions between electrons and carbon atoms.⁹ At the same time, the structural evolution of the tubes can be monitored *in situ* in the TEM. Moreover, as very recent experiments¹⁰ indicate, the TEM can detect the migration of even individual point defects. Monitoring the evolution of nanotubes under irradiation should also shed light on the production and dynamics of defects. Several TEM studies on irradiation-induced defects in carbon nanotubes have already been carried out,^{11–16} but many issues such as the dependence of the atom displacement threshold energy T_d on the tube diameter or the way how the tubes are actually destroyed—by sputtering or atom loss due to interstitial migration—remains open.

In this paper we provide experimental and theoretical evidence that MWNTs under electron irradiation are destroyed preferentially from inside due to a lower displacement threshold in the inner shells and migration of carbon atoms inside nanotubes. We show that carbon atoms can be trapped inside nanotubes and migrate in an axial direction through

the open core regions, because the diffusion on the outer surface of the tubes is hindered by a higher energy barrier.

MWNTs were grown in a conventional arc-discharge apparatus and collected on holey carbon grids for TEM studies. *In situ* electron microscopy was carried out in a FEI Tecnai F-30 with a field emission electron gun operating at 300 kV. To prevent the agglomeration of defects in the irradiated area,¹⁴ the specimens were held at temperatures around 600 °C in a heating stage (Philips). Small sections of the tubes were exposed to a focused electron beam of 10–25 nm diam. Beam current densities of 60–500 A/cm² were used. Alternatively, bundles of SWNTs were transformed to MWNTs by electron irradiation¹⁷ and then exposed to further irradiation.

Figure 1 shows the structural evolution of a MWNT under the electron beam. Intense irradiation (several hundred

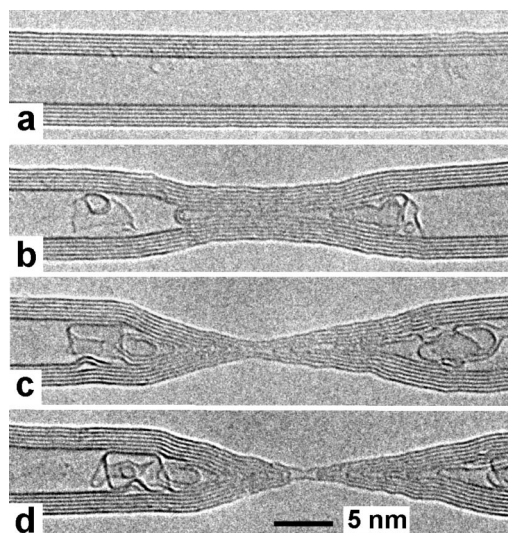


FIG. 1. Morphological evolution of a multiwalled carbon nanotube under electron irradiation. An electron beam with a diameter of 15 nm and a beam current density of approximately 450 A/cm² was focused onto the central part of the tube. The irradiation time: (a) $t=0$ (starting point); (b) $t=160$ s; (c) $t=340$ s; (d) $t=820$ s. The specimen temperature: 600 °C.

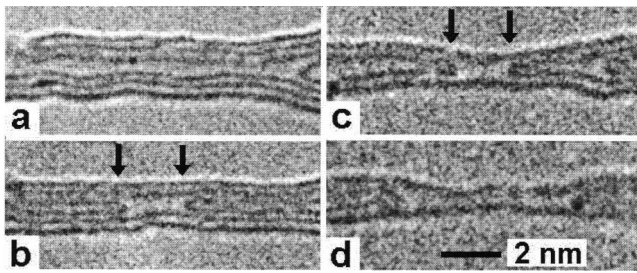


FIG. 2. Central part of a collapsing tube showing the successive loss of shells in detail. Electron beam diameter: 18–28 nm [increased deliberately from (a) to (d)]; corresponding beam current densities: 155–65 A/cm²; irradiation times: (a) $t=0$ (starting point); (b) $t=540$ s; (c) $t=1400$ s; (d) $t=2000$ s; specimen temperature: 600 °C. The three-shell tube in (a) was generated by transforming a bundle of SWNTs into a MWNT under electron irradiation. The caps closing the ends of the shells are arrowed.

A/cm²) leads to a shrinkage of all shells and collapse of the tube. Surprisingly, all shells remain temporarily intact (no breakage or disintegration) although material is lost (the surface area is decreasing). During the collapse, an aggregation of material in the shape of irregular graphitic cages occurs in the hollow core just outside the irradiated area [Figs. 1(b)–1(d)]. A rough estimate of the amount of material that has been lost during the collapse shows that the major fraction aggregates inside the tubes. Although a certain amount of material might be lost through the outermost layer, aggregation on the outer surface was never observed.

The initially cylindrical structure collapses into a morphology of a double cone (“hour glass”). Similar shapes of tubes have already been reported, but in a different context.¹⁸ As soon as the collapse is complete (the innermost tube has a diameter of a typical SWNT), an unexpected morphological evolution is observed (Fig. 2). Whereas the outer shells shrink but remain undamaged, the inner shells are successively broken until a SWNT in the center is left. It is always the innermost layer that breaks in such a way that the two halves form cones with closed caps. The cone from the innermost tube moves outwards (in the axial direction) and the cones from the other shells move up. Eventually, the last remaining shell breaks so that two separate multishell cones are left (not shown in the figures).

The evolution of a typical shrinking tube as a function of irradiation time is shown in Fig. 3. The outer diameter of the tube decreases rapidly until the inner hollow has collapsed and the channel is blocked by caps of the broken innermost tubes ($t=300$ s). Here, at a diameter of 1–2 nm (double or single wall), the tube remains surprisingly stable under further irradiation ($t=300$ –650 s); the loss of material is extremely small. Once the tube has shrunk below a diameter of 1 nm ($t>700$ s), the shrinkage proceeds faster again until the tube finally breaks ($t=850$ s).

From the observation of tens of MWNTs under irradiation, we can draw two conclusions: (i) The shrinkage of tubes proceeds faster when the inner hollow in the tube is open and large. As soon as the inner channel is closed by caps [Fig. 1(c)], the tubes show clearly increased stability

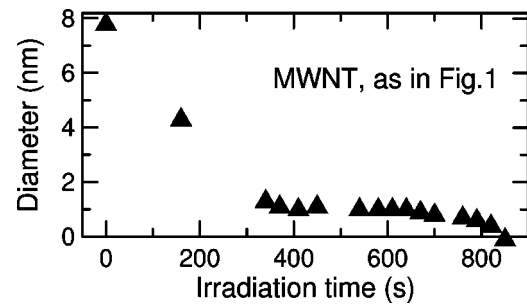


FIG. 3. Diameter of the nanotube shown in Fig. 1 as a function of irradiation time. The diameter of the outermost shell was measured in the center of the irradiated area where the arrangement has the lowest diameter. The irradiation conditions are as given in Fig. 1.

under the beam. (ii) The stability of tubes with diameters below 1–2 nm decreases with decreasing diameter.

To understand the stability of tubes in the presence or absence of an inner hollow, we have to treat as the first issue the migration of defects inside and outside of nanotubes. As experiments demonstrate, the migration barrier for vacancies in graphitic structures is higher than for interstitials,¹⁰ so that the interstitial diffusion should be much more important. To understand the diffusion of interstitials on the inner and outer surface of nanotubes, we can treat interstitials as carbon adatoms on the respective surfaces of SWNTs.¹⁹ We recently demonstrated²⁰ by tight-binding and plane-wave (PW) density functional theory (DFT) simulations that the migration barrier for carbon adatoms depends on the tube diameter, but it is always higher when the adatom is on the outer surface, as compared to the barrier for diffusion inside.

The mobility of adatoms inside SWNTs is highly affected by the curvature of the surface, especially in tubes with diameters less than 1 nm. The adatoms can easily spiral along the nanotube circumference with an energy barrier of 0.1–0.3 eV. The tight-binding calculations²⁰ showed that the barrier for migration inside the tube along the axis $E_m^{in} \sim 0.5$ eV is also much smaller than $E_m^{out} \sim 1$ eV (for a SWNT with the same diameter).

To get more quantitative data on E_m^{in} , we carried out PWDFT simulations of the diffusion of adatoms inside (5,5) and (6,6) tubes using the CASTEP (Ref. 21) code. As the migration path was known from our previous DFT-based tight-binding (DFTB) calculations, we evaluated the barrier by putting the adatom into different positions inside the tube and relaxing the system with constraints. A kinetic energy cutoff of 400 eV and up to six different \mathbf{k} points in the Brillouin zone made it possible to evaluate E_m^{in} with an accuracy of at least 0.1 eV. Our PWDFT simulations gave basically the same lowest energy geometry for the adatom and the same profile of the energy surface, but the barrier proved to be slightly less than the DFTB value: $E_m^{in} \approx 0.3$ eV. Thus, our *ab initio* simulations indicate that diffusion inside SWNTs is preferred against diffusion on the outer surface. Hence, if a carbon atom is displaced outwards and has not gained enough energy to leave the tube, the close separation from the vacancy and the high migration barrier should facilitate spontaneous reannealing so that the layer remains undam-

aged. Conversely, an adatom inside the layer has a higher mobility so that the escape of the atom in axial direction is facilitated.

The interstitials that are injected from the unstable inner shells vanish by axial diffusion through the tube. Once the innermost tube has shrunk to a diameter of approximately 0.5 nm, the lower stability limit is exceeded, the tube breaks, and conelike caps close the ends. When the caps are closed, the transport of material through the inner hollow is blocked, leading to a higher stability of the remaining tubes because interstitials are reflected back to the area under the beam where they are available for annealing with vacancies. Thus, the increased stability of small tubes with a closed inner hollow can be explained by the preferential diffusion of atoms inside the inner channel. This is also in line with the evolution of SWNTs under irradiation: We observe that the stability of the last SWNT in the collapsing arrangement under irradiation [Fig. 2(c)] is several times higher than of a typical long and open SWNT of the same diameter under the same irradiation conditions.

As the second issue, the stability of thin tubes as a function of their diameter (as seen from the final decrease of the curve in Fig. 3) can be due to an increasing rate of defect production with decreasing tube diameter. As shells in MWNTs weakly interact with each other due to a large separation, we can simplify the situation and consider interactions of energetic electrons with individual shells, i.e., SWNTs, to understand the differences in the defect production rate. It is well known^{9,12} that the primary cause of the electron irradiation damage in nanotubes are knock-on collisions of electrons with atomic nuclei. Thus, to get insight into defect production and the evolution of the tubes as shown in Fig. 2, we can treat the motion of atoms adiabatically and employ the nonorthogonal DFT-based tight-binding method²² we successfully used²⁰ to calculate properties of defects in SWNTs.

Firstly, we evaluated T_d by running free molecular dynamics, as in Ref. 12. We assigned a kinetic energy to a carbon atom in the graphene and nanotube network and simulated the evolution of the system. The initial momentum vector was perpendicular to the system surface, as such a configuration corresponds to the smallest escape energy.¹² We defined T_d as the minimum initial kinetic energy of the atom to escape from the system. We found that $T_d \approx 22$ eV for graphene. This is in line with, but somewhat larger than, the values of 15–20 eV reported in experimental studies⁹ for graphite.

Having evaluated T_d for flat graphene sheets, we calculated T_d for armchair SWNTs with chiral indices from 3 to 12. The upper curve in Fig. 4 shows T_d as a function of tube diameter for the initial momentum vector directed outwards from the SWNT. It is evident that for nanotubes with diameters of less than 1 nm, T_d quickly decreases as the tube diameter gets smaller with the difference between graphene and the smallest (3,3) SWNT considered being about 7 eV.

In a second simulation setup, we calculated T_d statically as $T_d = E(N+1) + E(N-1) - 2E(N)$, where $E(N)$ stands for the total energy of the perfect system composed of N atoms, and $E(N+1)$, $E(N-1)$ are the energies of the tube with adatom and vacancy, respectively. Physically, this expression gives

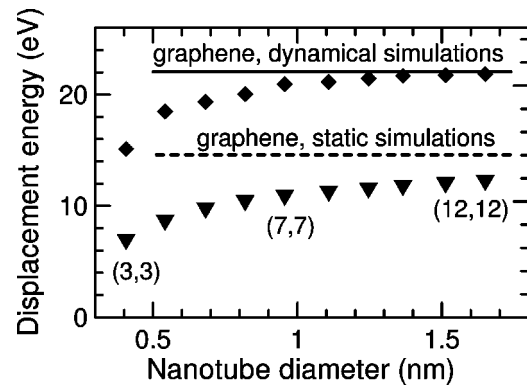


FIG. 4. Threshold energy T_d needed to displace carbon atoms from armchair single-walled carbon nanotubes and graphene calculated dynamically (diamonds) and statically (triangles) as a function of tube diameter. The lines are the corresponding results for graphene.

the energy of a spatially separated vacancy-interstitial pair.

Calculations for graphene gave $T_d \approx 15$ eV. This agrees with the experimental data, being on the lower side of the scatter. The dependence of T_d on the tube radius and the corresponding value for graphite are also shown in Fig. 4 (lower curve). Similar to the results obtained in the dynamical approach, T_d is much less for tubes with small diameters. The difference between graphene and a (3,3) SWNT also proved to be about 7 eV. The lower values of T_d for tubes with small diameters can be related to the curvature-induced strain in the nanotube atomic network.

The rate of atom displacements p is given by the product of the displacement cross-section σ and the beam current density j . For the present conditions, a displacement cross section of $\sigma = 30$ b was estimated by applying the McKinley-Feshbach formalism²³ and assuming a displacement threshold energy of $T_d = 15$ eV, which might be a realistic value for a larger tube [e.g., (12,12)]. For the series shown in Fig. 1, the following total numbers of displacements for each atom (dpa) were calculated by assuming the beginning of irradiation in Fig. 1(a): (a) 0 dpa (arbitrary starting point); (b) 13 dpa; (c) 29 dpa; (d) 69 dpa [in other words, each carbon atom was displaced 69 times in the irradiation period from (a) to (d)]. Assuming the qualitative behavior of the threshold energy as shown in Fig. 4 and the above-mentioned values valid for a (12,12) tube, the displacement rate in a (3,3) tube would be higher by approximately a factor of 1.7, whereas in a flat graphene sheet it would be slightly lower. Thus, the displacement rate is higher for the atoms in the inner shells. Extrapolating the data in Fig. 4 towards the diameter of large MWNTs with large hollows such as shown in Fig. 1(a) shows that there should be no substantial difference in displacement rates between the innermost and outermost shell. This is also observed experimentally: the initial shrinkage of the tube proceeds uniformly until the innermost shell has reached the diameter of a SWNT.

As follows from our analysis, the tubes are destroyed from inside due to the diffusion of interstitials via the inner core of the tubes (i) and a lower stability of smaller tubes (ii). Alternative scenarios such as a uniform mass loss of the

tubes by sputtering of atoms outwards and inwards cannot explain the results in Fig. 3. The curve would just show a kink when the inner hollow is filled and then continue with half of the initial slope. Atom displacements across more than 1 to 2 layers can be excluded from energy and momentum considerations. However, material exchange by diffusion across the layers should play a certain role and lead to annealing of vacancies in the intermediate layers and readjustment of their diameter to the outermost and innermost layers.²⁴ The van der Waals interaction between the shells appears to be large enough to prevent separation of the shells from each other due to different mass loss. Another argument against shrinkage by sputtering of atoms outwards is the observation of carbon onions (spherical multishell cages) under irradiation.⁹ Even under extremely intense electron beams, a surprisingly low sputtering-induced mass loss is observed (several times lower than in nanotubes). Unlike nanotubes, onions are completely closed and no possibility for internal mass loss exists.

To conclude, we have demonstrated that the threshold for displacing carbon atoms in carbon nanotubes and the defect production rate depend on the nanotube diameter because of the curvature-induced strain in the nanotube atomic network. We have also shown that carbon nanotubes under electron irradiation shrink by a loss of atoms inside the tubes and by diffusion of interstitials through the inner hollow in the axial direction. Therefore, we can consider carbon nanotubes as pipes for the effective transport of interstitial atoms. We can expect that foreign atoms or molecules are also highly mobile inside the hollow cores so that nanotubes appear ideally suited as pipelines on the atomic or molecular scale.

We acknowledge support from the Electron Microscopy Center Mainz (EMZM). We would like to thank Kai Nordlund for useful discussions. Grants of computer time from the Center for Scientific Computing in Espoo, Finland are gratefully acknowledged.

-
- ¹ *Carbon Nanotubes, Synthesis, Structure, Properties and Applications*, edited by M. S. Dresselhaus, G. Dresselhaus, and P. Avouris (Springer, Berlin, 2001).
- ² A. C. Dillon, K. M. Jones, T. A. Bekkedahl, C. H. Kiang, D. S. Bethune, and M. J. Heben, *Nature (London)* **386**, 377 (1997).
- ³ G. E. Gadd, M. Blackford, S. Moricca, N. Webb, P. J. Evans, A. M. Smith, G. Jacobsen, S. Leung, A. Day, and Q. Hua, *Science* **277**, 933 (1997).
- ⁴ V. Meunier, J. Kephart, C. Roland, and J. Bernholc, *Phys. Rev. Lett.* **88**, 075506 (2002).
- ⁵ Z. Mao and S. B. Sinnott, *Phys. Rev. Lett.* **89**, 278301 (2002).
- ⁶ G. Hummer, J. C. Raisaiah, and J. P. Noworyta, *Nature (London)* **414**, 188 (2001).
- ⁷ A. I. Skoulidas, D. M. Ackerman, J. K. Johnson, and D. S. Sholl, *Phys. Rev. Lett.* **89**, 185901 (2002).
- ⁸ D. Cao and J. Wu, *Langmuir* **20**, 2739 (2004).
- ⁹ F. Banhart, *Rep. Prog. Phys.* **62**, 1181 (1999).
- ¹⁰ A. Hashimoto, K. Suenaga, A. Gloter, K. Urita, and S. Iijima, *Nature (London)* **430**, 870 (2004).
- ¹¹ C.-H. Kiang, W. A. Goddard, R. Beyers, and D. S. Bethune, *J. Phys. Chem.* **100**, 3749 (1996).
- ¹² V. H. Crespi, N. G. Chopra, M. L. Cohen, A. Zettl, and S. G. Louie, *Phys. Rev. B* **54**, 5927 (1996).
- ¹³ N. G. Chopra, F. M. Ross, and A. Zettl, *Chem. Phys. Lett.* **256**, 241 (1996).
- ¹⁴ F. Banhart, T. Füller, P. Redlich, and P. M. Ajayan, *Chem. Phys. Lett.* **269**, 349 (1997).
- ¹⁵ P. M. Ajayan, V. Ravikumar, and J.-C. Charlier, *Phys. Rev. Lett.* **81**, 1437 (1998).
- ¹⁶ B. W. Smith and D. E. Luzzi, *J. Appl. Phys.* **90**, 3509 (2001).
- ¹⁷ J. X. Li and F. Banhart, *Nano Lett.* **4**, 1143 (2004).
- ¹⁸ H. E. Troiani, M. Miki-Yoshida, G. A. Camacho-Bragado, M. A. L. Marques, A. Rubio, J. A. Ascencio, and M. José-Yacaman, *Nano Lett.* **3**, 751 (2003).
- ¹⁹ This is possible in part due to relatively large separations between graphitic shells in nanotube samples.
- ²⁰ A. V. Krasheninnikov, K. Nordlund, P. O. Lehtinen, A. S. Foster, A. Ayuela, and R. M. Nieminen, *Phys. Rev. B* **69**, 073402 (2004).
- ²¹ V. Milman, B. Winkler, J. A. White, C. J. Pickard, M. C. Payne, E. V. Akhmatkaya, and R. H. Nobes, *Int. J. Quantum Chem.* **77**, 895 (2000).
- ²² T. Frauenheim, G. Seifert, M. Elstner, T. Niehaus, C. Köhler, M. Amkreutz, M. Sternberg, Z. Hajnal, A. Di Carlo, and S. Suhai, *J. Phys.: Condens. Matter* **14**, 3015 (2002).
- ²³ W. A. McKinley and H. Feshbach, *Phys. Rev.* **74**, 1759 (1948).
- ²⁴ C. H. Kiang, M. Endo, P. M. Ajayan, G. Dresselhaus, and M. S. Dresselhaus, *Phys. Rev. Lett.* **81**, 1869 (1998).